We are IntechOpen,
the world's leading publisher of
Open Access books
Built by scientists, for scientists

6,900
Open access books available

186,000
International authors and editors

200M
Downloads

154
Countries delivered to

Our authors are among the

TOP 1%
most cited scientists

12.2%
Contributors from top 500 universities

BOOK CITATION INDEX
CLARIVATE ANALYTICS
INDEXED

WEB OF SCIENCE™

Selection of our books indexed in the Book Citation Index
in Web of Science™ Core Collection (BKCI)

Interested in publishing with us?
Contact book.department@intechopen.com

Numbers displayed above are based on latest data collected.
For more information visit www.intechopen.com

5

Life Span of Biopolymer Sequestering Agents for Contaminant Removal and Erosion Resistance

Anna Sophia Knox[1], Ioana G. Petrisor[2], Charles E. Turick[1], Jesse Roberts[3],
Michael. H. Paller[1], Danny. D. Reible[4], and Casey R. Forrest[4]
[1]Savannah River National Laboratory
[2]Haley&Aldrich, Inc.
[3]Sandia National Laboratories
[4]University of Texas
United States of America

1. Introduction

The objective of this paper is to report the development and life span of cross-linked biopolymers that remove contaminants, resist biodegradation over long periods of time, and resist erosion in dynamic aquatic environments.

Biopolymers are polymeric compounds produced by living organisms (e.g., microorganisms, plants, crustaceans). They have repeated sequences that vary broadly in chemical composition including a variety of repeating functional groups (such as carboxyl, hydroxyl, amino, etc.). This makes them reactive and subject to cross-linking. Therefore, biopolymers, a great molecular weight compounds with repeated sequences, may have high opportunity for chemical interaction with other compounds. Depending on their functional groups, biopolymers can bind metals, organic contaminants, or soil particles and form interpenetrating cross-linking networks with other polymers. The ability of biopolymers (cross-linked or not) to bind a large variety of metals is supported by many studies (Chen et al., 1993; Etemadi et al., 2003; Knox et al., 2008 a, b). The capacity of alginate as a cross-linked product (calcium alginate) for Cr(VI) uptake was demonstrated by Fiol et al. (2004), who obtained an uptake of 86.42 mmol of Cr(VI) per L of wet sorbent volume using grape stalk wastes encapsulated into calcium alginate. The Cr(VI) removal ability of cross-linked calcium alginate was also shown by Araujo and Teixeira (1997), and its ability to bind Cu was shown by Chen et al. (1990 and 1993) and Wan et al. (2004). The removal of Cu, Cr, and As from treated wood onto the biopolymers, chitin and chitosan, was shown by Kartal and Iamamura (2004). The use of biopolymers based on elastine-like polypeptides for the selective removal of Hg was reported by Kostal et al. (2003), who also reported their potential for binding and removal of other metals such as As and Cr. Recently, the use of a similar elastin-like polypeptide composed of a polyhistidine tail was exploited as a metal-binding biopolymer with high affinity toward Cd by Prabhukumar et al. (2004). Knox et al. (2007 and 2008 a, b) showed that biopolymers (with and without cross-linking) have the ability to sequester a large variety of metals (e.g., Cu, Pb, Cd, As, Cr, Zn, and Ni) and organic contaminants (e.g., phenanthrene and pyrene).

Apart from their contaminant binding ability, the use of biopolymers as plugging agents is well known. They are easily introduced in subsurface environments by injection under pressure using drilling equipment similar to that in the oil industry. Several studies (Yen et al., 1996; Stewart and Fogler, 2001; Khachatoorian et al., 2004) reported the application of biopolymers and associated microorganisms as plugging agents to construct a range of impervious barriers. Apart from their plugging effect, biopolymers can bind metals, soil/sediment particles and other biopolymers with the added ability to create cross-linking interpenetrating networks that may encapsulate contaminants into very stable forms as geopolymers (Kim et al, 2004 and 2005). Subsequently, the application of biopolymers to soils or sediments may result in the formation of barriers that isolate the contaminants, with possible permanent encapsulation of some contaminants and fixation of soils or sediments thereafter.

Cross-linking is the process of chemically joining two or more molecules by a covalent or ionic bond using a cross-linking agent (or cross-linker). Cross-linkers contain at least two reactive groups (identical or different). Functional groups that can be targeted for cross-linking include primary amines, sulfhydryls, carbonyls, carbohydrates, and carboxylic acids (most of these groups are possessed by biopolymers). Coupling also can be nonselective using a photoreactive phenyl azide cross-linker. Cross-linked biopolymers should become resistant to biodegradation and have the potential for remedial applications. As a result of the cross-linking process the biopolymer molecular mass increases. Many additional bonds are created between the biopolymer chains inside the cross-linked network, which makes an enzymatic attack (brake in the chain) less or even non- effective in terms of changes in the molecular weight of the whole cross-linked product. Cross-linking agents are used to enhance the strength of polymers and to decrease their biodegradability. Cross-linking agents are chosen based on the functional groups of polymers. The interpenetrating polymer networks (IPNs) developed by cross-linking may stop or slow the migration of contaminants as a result of increased viscosity, reduced permeability of porous media, and greater stablility at lower pH values.

In this study commercially available biopolymers were treated with cross-linking agents to produce cross-linked biopolymers that stabilize contaminants in soil or sediments while improving soil/sediment structure to reduce physical processes (e.g., erosion) that result in contaminant dispersal. Sediment and aqueous environments contaminated with heavy metals and organic contaminants remain a serious concern worldwide. New technologies focusing on permanent methods of in situ enclosure of contaminants effectively reducing risk levels to acceptable levels are currently being developed; one of them is capping technology. Capping technology is one of the few in-situ technologies available to environmental scientists and engineers to remediate polluted sediments in aquatic environments. Conventional capping technology usually employs sand as a cap, which may provide inadequate risk reduction at some sites. An alternative to a passive plain-sand cap is to directly amend the sand to provide a more sorptive medium to retain contaminants and further retard their transport from the sediment into the benthic zone and water column (Palermo et al., 1998). Retardation of the migrating contaminants serves a two-fold benefit. Not only are contaminants withheld from the overlying water column but their increased retention time in the sediment allows for natural attenuation processes to more fully degrade and reduce the associated hazards. Increased retention time allows for the deposition of clean sediment on top of the cap as well as more effective progress by the slower biodegradation processes.

Active caps, or permeable adsorptive barriers, are being developed and implemented as an alternative, cost effective remediation technology. Active capping involves the use of capping materials that are reactive and not only isolate but also sequester contaminants, further preventing their mobility, toxicity, and bioavailability (Knox et al., 2006, 2007, and 2008 a and b). Active capping technologies currently lay at the forefront of contaminated river sediment remediation techniques and research. Innovative capping technologies need to be explored to enhance the capabilities of a sand cap (Reible et al., 2006). Biopolymer materials composed, for example, of chitosan, xanthan gum, and guar gum may be a promising addition to materials for active capping technology due to greater organic content than in a conventional sand cap and therefore better sorption-related retardation. Also, the repeated sequences exhibited by biopolymers provide ample opportunity for chemical reactions with metals and sediment particles, allowing for the effective containment of contaminants.

Previous research suggests that cross-linked biopolymers are stable in soil, and that stability may increase over time, in some cases entrapping contaminants in stable geological structures such as geopolymers. However, the stability of biopolymers and their anticipated life span may be affected by environmental conditions indicating a need for further evaluation before this technology is deployed for remediation of contaminated soils or sediments. Biopolymers such as xanthan gum and chitosan are used extensively in industry resulting in substantial information concerning their biogdegradaability. Xanthan gum is not easily degraded by microorganisms (Cadmus et al., 1982), and chitosan polymers have antimicrobial activities. Interestingly, partially degraded chitosan demonstrates enhanced antimicrobial activities (Rhodes and Roller 2000). While biopolymer biodegradation is enhanced by elevated temperature and salt concentrations, metals sorbed to organic chelators can significantly decrease their rate of biodegradation (Francis and Dodge, 1993).

In this study biopolymers were evaluated for metal and organic contaminant removal, alone and in combination with soil/sediment, as potential candidate materials in active capping applications. This evaluation included the assessment of stability over time under varying environmental conditions (e.g., elevated temperature and moisture). Also evaluated were microbial effects on the properties of cross-linked biopolymers, and long term effects of selected cross-linked biopolymers on the mobility and retention of contaminants in sediments. Commercially available biopolymers that were evaluated in these laboratory studies included chitosan, xanthan, guar gum, and alginate. Cross-linking agents for these biopolymers included borax, xanthan, and calcium chloride. Since erosion control is a big part of successful remedial technology for contaminated sediments, e.g., active capping, the selected biopolymers were tested (as a slurry or coated on sand particles) for erosion resistance in the lab.

2. Materials and methods

Development of cross-linked biopolymer and biopolymer coated sand or sand/amendments is presented in Tab. 1 and 2. The most promising products, which had high carbon fractions (indicating greater coverage of biopolymer) and high viscosity were evaluated further for metal and organic sorption, biodegradability, and resistance to physical disturbance/erosion.

2.1 Sorption of metals on biopolymers
Xanthan crossed linked with guar gum and xanthan cross-linked with chitosan were evaluated for metal removal in a sorption study (Tab. 1). The experiments were conducted

in 50 mL centrifuge tubes for one week. Each treatment had three replicates. The spike solution used in the experiment was obtained from Inorganic Ventures, Lakewood, NJ. The metal concentrations in the spike solution were 5 mg L^{-1} of As, Cd, Cr, Co, Cu, Pb, Ni, Se, and Zn. Suspensions composed of 0.2 gram of solid and 15 mL of spike solution were shaken for one week, phase separated by centrifugation, and then analyzed for metals by inductively coupled plasma – mass spectrometry (ICP-MS).

Major Product Name	Primary Biopolymers	Cross-link Agent	Modified Product name	Biopolymer Sand ratio	Additives			
					5% HCl	Glutar-aldehyde	1N NaOH	water
					mL	mL	mL	mL
CGB	Chitosan Guar gum	Borax	CGB1	0.05	475			500
			CGB2	0.05	200	5		300
			CGB3	0.05	200		20	400
GB	Guar gum	Borax	GB1	0.005	100			500
			GB2	0.005			20	600
			GB3	0.025		5	20	600
GX	Guar gum	Xanthan	GX1	0.05	100			500
			GX2	0.05			20	600
			GX3	0.05				500
XCc	Xanthan Chitosan	Calcium chloride	XCc	0.025	100	5		500
XC	Xanthan	Chitosan	XC					500
XG	Xanthan	Guar gum	XG					500

Table 1. Biopolymer products that were used for sand coating and contaminant sorption.

2.2 Sorption of organic contaminants on biopolymers

Sand samples coated with chitosan/guar gum cross-linked with borax (CGB3) and with xanthan/chitosan cross-linked with calcium chloride (XCc) were evaluated for their capacity to sorb organic contaminants (Tab. 1). PAHs used in this study were purchased from a commercial supplier (Sigma Aldrich, MO). They included 5000 µg L^{-1} phenanthrene in methanol, 1000 µg L^{-1} pyrene in methanol, and 200 µg L^{-1} benzo(a)pyrene in methylene chloride. These solutions were diluted in electrolyte solutions (0.01M NaCl, 0.01M CaCL$_2$.2H$_2$O) to prepare a mixture of 20 µg L^{-1} phenanthrene and 100 µg L^{-1} pyrene. Exact concentrations of these compounds were determined by high performance liquid chromatography (HPLC) affiliated with a Waters 2475 Multi λ Fluorescence Detector and Waters 996 Photodiode Array Detector. Sodium azide (0.05M) was added to the electrolyte solution to inhibit bacterial degradation of the PAHs.

2.3 Stability of cross-linked biopolymers under varying environmental conditions
2.3.1 Biodegradability of biopolymers

Biopolymer products were evaluated for biodegradability by microorganisms associated with the polymers. One gram of polymer material was mixed with and without 10 ml sterile basal salts medium (BSM) (Turick et al. 2002) and sealed in sterile test tubes with airtight

Product Number	Coated Sand	Biopolymers/ Cross-link Agent	Preparation Method
1	CGB	Chitosan / Guar Gum/ Borax	2 kg sand + 50 g guar gum + 50 g chitosan + 25 g borax + 300 mL 1N NOH + 6 L tap water Sand, biopolymer powders, and cross-link agent were well mixed as solids. One N NaOH was added to create a basic pH for cross-linking of guar with borax. Water was added in small amounts under continuous shaking, followed by the addition of acid under continuous shaking. The prepared material was placed on a rotary shaker (at about 30-40 rpm) overnight (12 h), then neutralized by the addition of 1N NaOH. The coated sand (as slurry) was collected wet and stored wet for erosion testing.
4*	XCc	Xanthan/ Chitosan / Calcium chloride/ glutaral-dehyde	2 kg sand + 50 g xanthan + 50 g chitosan + 15 g CaCl$_2$ + 75 mL glutaraldehyde + 6 L tap water Sand, biopolymer powders, and cross-link agent CaCl$_2$ were well mixed as solids, then 50 mL glutaraldehyde was added. Additional mixing was performed mechanically. Water was added in small amounts under continuous shaking. The prepared material was left on a rotary shaker (at about 30-40 rpm) overnight (12 h), after which the pH was adjusted to neutral and the mixture filtered through a sieve. The coated sand (as slurry) was collected wet and stored for erosion testing.
5*	XG	Guar Gum/ Xanthan	2 kg sand + 25 g guar gum + 25 g xanthan + 6 L tap water Sand and biopolymer powders were well mixed as solids. Water was then added under continuous shaking. The prepared material was placed on a rotary shaker (at about 30-40 rpm) overnight (12 h). The coated sand (as slurry) was collected wet and stored wet for erosion testing.
6*	XG		2 kg sand + 50 g guar gum + 50 g xanthan + 6 L tap water The same procedure as product #5.
7*	AXG	Guar Gum/ Xanthan/ NC apatite	1.75 kg sand + 0.25 kg apatite + 50 g guar gum + 50 g xanthan + 6 L tap water The same procedure as product #5.
8*	OXG	Guar Gum/ Xanthan/ PM-199 organoclay	1.75 kg of sand + 0.25 kg of organoclay + 50 g guar gum + 50 g xanthan + 6 L tap water The same procedure as product #5.
9*	XG/AO	Guar Gum/ Xanthan/ NC apatite/PM-199 Organoclay	1.5 kg of sand + 0.25 apatite + 0.25 kg of organoclay + 50 g guar gum + 50 g xanthan + 6 L tap water The same procedure as product #5.

Table 2. Preparation methods for biopolymers and biopolymer coated sand materials. Materials selected for erosion tests in an Adjustable Shear Stress Erosion and Transport (ASSET) flume are marked by an asterisk.

butyl rubber stoppers. Uncoated sand was used as a control for comparison with the biopolymer coated sand. Static incubation in the dark was at 0°C and 35°C. Low temperature (0°C) and high temperature (35°C) and wet and dry moisture regimes simulated a broad range of environmental conditions and seasonal changes. Microbial activity (biopolymer degradation) was measured by CO_2 release with a Hewlett Packard 5890 series 2 gas chromatograph (GC) with a mass spectrometer. A 250 µl sample of the headspace gas was injected into the GC using a gas tight syringe with a side-hole needle. A carrier gas of helium was used to move the sample through the column into the mass spectrometer. An internal standard of argon was used to calculate CO_2 production in the samples. The release of CO_2 from the biopolymer coated sands was measured for ten weeks. Additionally, metal concentrations for biopolymers from the sorption experiment were also evaluated (ICP/MS) upon termination of this experiment in an effort to correlate biopolymer breakdown with metal release. Microbial density on biopolymers was characterized at the termination of the study by direct microscopic counts. Filtered biopolymers and cells were stained with 496-diamidino-2-phenylindole (DAPI), and stained cells were detected using epifluorescent illumination (Lehman et. al 2001). The heterogeneous nature of the biopolymers did not permit quantitative enumeration of cells, but results generally correlated with CO_2 evolution.

2.3.2 Microbial effects on the properties of biopolymers

Microbial degradation of the biopolymers was further evaluated by sampling polymers that appear to be biodegradable (as indicated by increased CO_2 evolution) by soil microbes. This method included addition of sterile biopolymers to BSM or BSM solidified with 1.5% Noble agar, thus providing the biopolymers as the sole source of carbon for microbial isolates associated with the biopolymers (above). As a source of bacterial inocula, fresh sediment was treated following the methods of Lehman et al. (2001), which included addition of 0.1% sodium pyrophophate, and blended followed by sedimentation (for 24 hrs) of sediment particles. Disorbed bacteria, in suspension, were used as inocula for degradation studies following washing in phosphate buffer. A 1% inoculun (wt/vol) was added to sterile biopolymers in gas tight vials as above. Carbon dioxide evolution and oxygen utilization were monitored over time to determine the rate (if any) of degradation. Controls consisted of uninoculated biopolymers as well as inoculum without biopolymers. The samples were incubated statically in the dark for 2 weeks at 25°C to evaluate microbial growth resulting from biopolymer breakdown. Gas analyses were conducted either through periodic GC headspace analysis or via respirometry. Following the incubation period (when CO_2 concentrations level off), biopolymer material was dried and weighed to determine loss due to biodegradation, and a carbon balance was attempted with the CO_2 data. Microbial isolates were grown with specific polymers (i.e., guar gum, chitosan, glutaraldehyde, etc.) on BSM and Nobel agar plates to obtain a gross characterization of microbial community changes resulting from polymer biodegradation. Growth did not occur on Nobel agar plates without supplemental carbon. Biopolymers were also evaluated before and after degradation using electron microscopy to determine if biodegradation affected polymer size. Polymer breakdown products were evaluated by ion chromatography and/or GC/MS.

2.4 Evaluation of biopolymer resistance to physical disturbance

The resistance of biopolymers to physical disturbance was evaluated by shaker tests and by an Adjustable Shear Stress Erosion and Transport (ASSET) flume.

2.4.1 Evaluation of suspension by shaker tests

The biopolymer materials tested for erosion resistance and methods for preparing biopolymer products are described in Tab. 2. These products were prepared and kept wet (as a slurry) for testing as a wet product. Two -5 kg of each product were produced. The main objective of this study was to identify biopolymer products that could resist erosion.

A standard shaker test (Tsai and Lick, 1986) was used to assess the ability of sand and amendments with and without biopolymers to resist physical disturbance. The shaker allowed a standardized assessment of the shear stress needed to suspend a sample. The shear stress needed to suspend a sample was measured using a sampling port (Fig. 1). Seven cm of sample was placed inside of the cylindrical chamber, and sufficient distilled water was added to the cylinder to bring the depth to 12.7 cm. Suspended sample particles were allowed to settle, the cylinder was reattached to the shaker, and the motor speed was recorded when the following conditions were visually observed: fine top particles disturbed, motion of top particles, cloudiness, full re-suspension of top layer, and full re-suspension of bottom layer. The motor speed of the shaker drive disc was measured with a tachometer in meters per minute. The circumference of the drive disc (17 cm) was measured and used to convert the m/min measurements into revolutions per minute (0.17 rpm), which was further converted to oscillations by the following equation (equation 1)

$$oscillation period = \frac{1}{60 \times RPM} \qquad (1)$$

Fig. 1. Shaker for simulating erosion.

2.4.2 Evaluation of erosion by Adjustable Shear Stress Erosion and Transport (ASSET) flume

2.4.2.1 Description of the ASSET flume

The ASSET flume is considered a next generation SEDflume in that it maintains all capabilities of its predecessor while also quantifying the transport modes of the sediments after erosion. The erosion test section of the ASSET flume is similar in design, with a slightly taller channel height, and identical in erosion testing operation to the SEDflume, which has been described extensively in the literature (McNeil et al., 1996; Jepsen et al., 1996; Roberts et al., 1998; Jepsen et al., 1997; Roberts and Jepsen, 2001). It consists of eight primary components (Fig. 2): a 120 gallon reservoir, a 200 gpm centrifugal pump, a motor controlled screw jack, an erosion channel including erosion test section, a transport channel including bedload traps, a three way valve, a magnetic flow meter, and connective plumbing. Water is pumped from the reservoir through the three-way valve, which either sends water directly back to the reservoir or through the flow meter to the erosion and transport channels (and then back to the reservoir). A manually controlled screw jack is used to push the sediments through the core tube to keep the sediment surface flush with the channel floor such that, as closely as possible, the sediments are exposed only to an applied shear stress.

The ASSET Flume's enclosed (internal flow) erosion and transport channels are 5 cm tall and 10.5 cm wide (Fig. 2). The erosion test section is preceded by 180 cm of enclosed rectangular channel to ensure fully developed turbulent flow over the sediment core. The cylindrical sediment core tube is 10 cm in diameter. The first bedload trap is located 1m from the center of the erosion test section, and the center of each successive trap is 1 m from the center of the preceding one. Based on the theoretical definition of bedload in combination with fluid velocities and particle/aggregate settling speeds, a bedload particle/aggregate should contact the flume floor at least once every 15 cm of downstream travel. Consequently, the traps are 15 cm long and span the width of the channel (10.5 cm). Capture basins that are 10 cm deep and have a 2 L volume are located below the traps, each with a baffle system that reduces recirculation and minimizes the resuspension of trapped sediments. As the sediment core is eroded upstream, some of the material is suspended and some is transported as bedload. All sediment that falls into the traps is considered bedload.
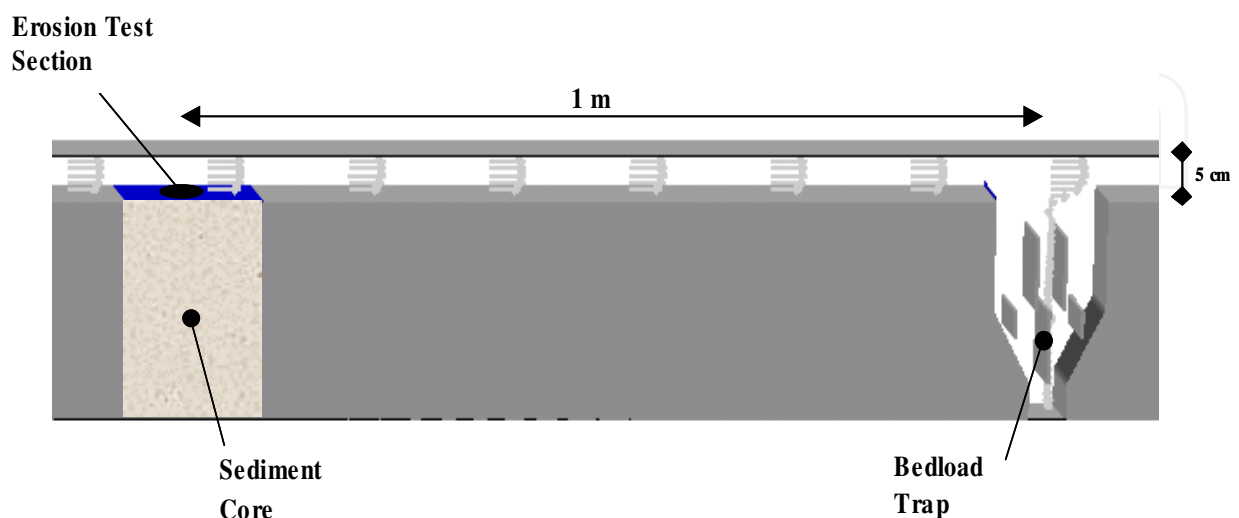

Fig. 2. Schematic of the ASSET flume.

2.4.2.2 Hydrodynamics

The hydrodynamics within the flow channel of the ASSET Flume are equivalent to those of the SEDflume (McNeil et al., 1996); however, the increase in duct height necessitated a change to the system inlet. To achieve fully developed turbulent flow over the sediment core, the flume inlet was lengthened to 180 cm and preceded by a 20 cm circular-to-rectangular flow converter and several meters of inlet pipe. Turbulent flow through pipes has been studied extensively, and empirical functions have been developed that relate the mean flow rate to the boundary shear stress. In general, flow in circular cross-section pipes has been investigated. However, the relations developed for flow through circular pipes can be extended to non-circular cross-sections by means of a shape factor. An implicit formula relating the boundary shear stress to the mean flow in a pipe of arbitrary cross-section can be obtained from Prandtl's Universal Law of Friction (Schlichting, 1979). For a pipe with a smooth surface, this formula is

$$\frac{1}{\sqrt{\lambda}} = 2.0 \log\left[\frac{UD\sqrt{\lambda}}{\nu}\right] - 0.8 \tag{2}$$

where U is the mean flow speed, ν is the kinematic viscosity, λ is the friction factor, and D is the hydraulic diameter. For a duct with a rectangular cross-section the hydraulic diameter is

$$D = 2hw/(h + w) \tag{3}$$

where w is the duct width and h is the duct height. The friction factor is defined as

$$\lambda = \frac{8\tau}{\rho U^2} \tag{4}$$

where ρ is the density of water and τ is the wall shear stress. Substituting Eqs. (3) and (4) into Eq. (2) yields the boundary shear stress as an implicit function of the mean flow speed. The mean flow speed and hence the boundary shear stress are controlled by the pump speed. For flow in a circular pipe, turbulent flow theory suggests that the transition from laminar to fully turbulent flow occurs within 25 to 40 diameters from the entrance to the pipe. Because the hydraulic diameter of the duct is 6.8 cm, this indicates a necessary entry length between 170 and 270 cm, which is supplied by the inlet piping, converter, and ducting. Furthermore, for shear stresses in the range of 0.1 to 10 N/m^2, the Reynolds numbers, UD/ν, are on the order of 10^4 to 10^5 implying that turbulent flow existed in all experiments performed for this study. These arguments along with direct observations indicate that the flow is fully turbulent in the test section.

2.4.2.3 Sample collection and preparation for the ASSET flume Test

Samples tested in the ASSET flume were prepared following the method described in Tab. 2. All materials were stored in a refrigerator at 4°C. The samples were stirred and poured into erosion core tubes to a depth of 10 cm. Five cm of water was gently poured on top of each material, which was returned to a refrigerator. Each sample remained in the refrigerator until the day of the erosion test for consolidation times of 2, 5, 10, and 175 days.

2.4.2.4 Measurements of sediment erosion rates and critical shear stress

To measure the erosion rates of the samples as a function of shear stress and depth, the samples were placed upward into the test section until the sample surface was even with the bottom of the test section. A measurement was made of the depth to the bottom of the sample in the tube. The flume was then run at a specific flow rate corresponding to a particular shear stress. Erosion rates were obtained by measuring the remaining sample depth at different time intervals, taking the difference between each successive measurement, and dividing by the time interval.

To measure erosion rates at several different shear stresses using only one sample, the flume was run sequentially at higher shear stresses with each succeeding shear stress being 1.33, 1.5 or 2 times the previous one. Generally between three and five shear stresses were run sequentially. Each shear stress was run until at least 0.5 mm but no more than 10 mm were eroded. The time interval was recorded for each run with a stop watch. The flow was then increased to the next shear stress, and so on until the highest shear stress was run.

A critical shear stress can be quantitatively defined as the shear stress at which a very small, but accurately measurable rate of erosion occurs. In the present study, this rate of erosion was chosen to be 10^{-4} cm/s; this represents 1 mm of erosion in approximately 15 minutes. Since it would be difficult to measure all critical shear stresses at exactly 10^{-4} cm/s, erosion rates were generally measured above and below 10^{-4} cm/s at shear stresses which differ by a factor of 1.33, 1.5 or 2. The critical shear stress was then linearly interpolated to an erosion rate of 10^{-4} cm/s. This gave results with 20% accuracy for determination of critical shear stress.

2.4.2.5 Erosion rate ratio analysis

The erosion rate data collected for each sample is generally plotted as erosion rate as a function of depth from the sediment surface and applied shear stress. The non-linear relationship between erosion rate and bed shear stress can make it difficult to quantify variability in the erosion behavior within a single core and between many cores. In order to overcome this limitation, the data can be analyzed to determine an erosion rate ratio that produces a single numerical value for a particular erosion rate data series that accounts for this non-linear relationship (Jones et. al, 2008). The erosion rate ratio is used to make direct comparisons between erodibility within a single core (i.e. to identify changes with depth), between similar cores, and between all tested cores to aid in the identification of the most erosion resistant cap material.

In this analysis, each core was sub-sampled into separate depth intervals. Following the methods of Roberts et al (1998), the erosion rate for each depth interval can be approximated by a power law function of sediment density and applied shear stress. For a particular depth interval, density is assumed to remain relatively constant, therefore the density term is dropped. For each depth interval, the measured erosion rates (E) and applied shear stresses (τ) are used to develop the following equation.

$$E = A\tau^n \qquad\qquad (5)$$

Where E is the erosion rate (cm/s) and τ is shear stress (Pa). The parameters A and n are determined using a log-linear regression analysis. From this analysis an average erosion rate for the entire core can also be determined, and the erosion rate at each depth interval can be directly compared to this average. The result is an erosion rate ratio which provides an estimation of the erosion susceptibility of each depth interval relative to the core average. In

addition, an average erosion rate of similar core and for all cores can be determined. The erosion rate for each depth interval within a core as well as each cores average erosion rate can be compared to the specified average and a graph of the erosion rate ratios for all of the cores can be created and compared to the average erosion behavior of all cores.

3. Results and discussion

3.1 Sorption of metals and organic contaminants by biopolymers

The most promising materials for metal removal were xanthan crossed linked with guar gum and xanthan cross-linked with chitosan (Fig. 3). These cross-linked biopolymers sequestered a variety of metals from a spike solution; e.g., As, Cd, Co, Cr, Cu, Ni, Pb, and Zn (Fig. 3). Removal of most metals by xanthan crossed linked with guar gum and xanthan cross-linked with chitosan exceeded 90% (Fig. 3). The tested biopolymers were as effective at removing metals from the spike solution as apatite (rock phosphate from North Carolina), which has proven ability to immobilize metals such as Pb, Cd, and Zn in soils and sediments (Knox et al, 2008a) (Fig. 3).

Various processes such as adsorption, ion exchange, and chelation dominate the mechanisms responsible for complex formation between biopolymers and metal ions. The interactions of metal ions with biopolymers (e.g., chitosan) also are influenced by the degree of polymerization and deacetylation, as well as by the distribution of acetyl groups along the polymer chains (Bassi et al., 1999). The evidence currently available supports the concept that chitosan-metal ion complex formation occurs primarily through the amino groups functioning as ligands (Udaybhaskar et al., 1990; Randall et al., 1979).
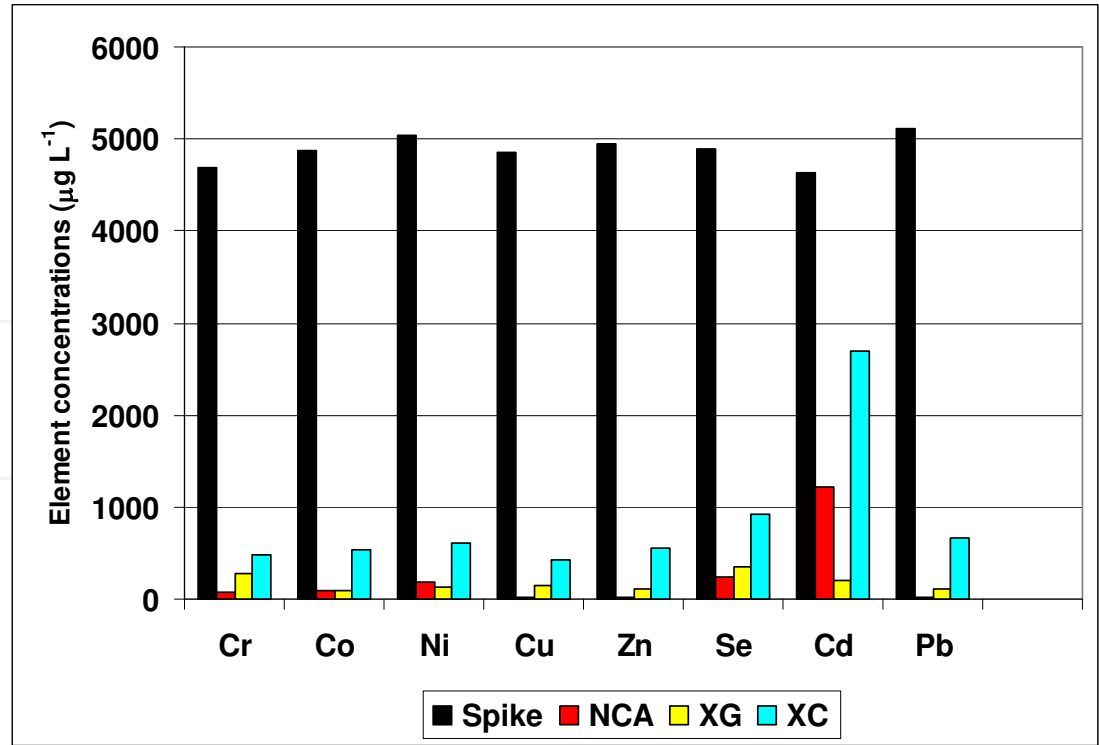
Fig. 3. Removal of metals by biopolymers from a spike solution with an initial concentration of 4800 µg L^{-1} of As, Cd, Co, Cr, Cu, Ni, Pb, Se, and Zn; NCA - North Carolina apatite, XG - xanthan cross-linked with guar gum, XC - xanthan cross-linked with chitosan.

Organic carbon content was measured as an indicator of the efficiency of the procedure for coating the sand with biopolymers and as an indicator of the potential for the sorption of organic contaminants on the coated sand. The measured carbon fractions are presented in Fig. 4. The carbon fractions of coated sand with one wash, two washes and three washes did not differ substantially from the unwashed sand, indicating that the coated sand was resistant to washing.

Sorption capacities of sand samples coated with chitosan/guar gum cross-linked with borax (CGB) and with xanthan/chitosan cross-linked with calcium chloride (XCc) are presented in Tab. 3. Both biopolymer coated sand materials had a significantly higher soption capability than sand for pyrene (Tab. 3).
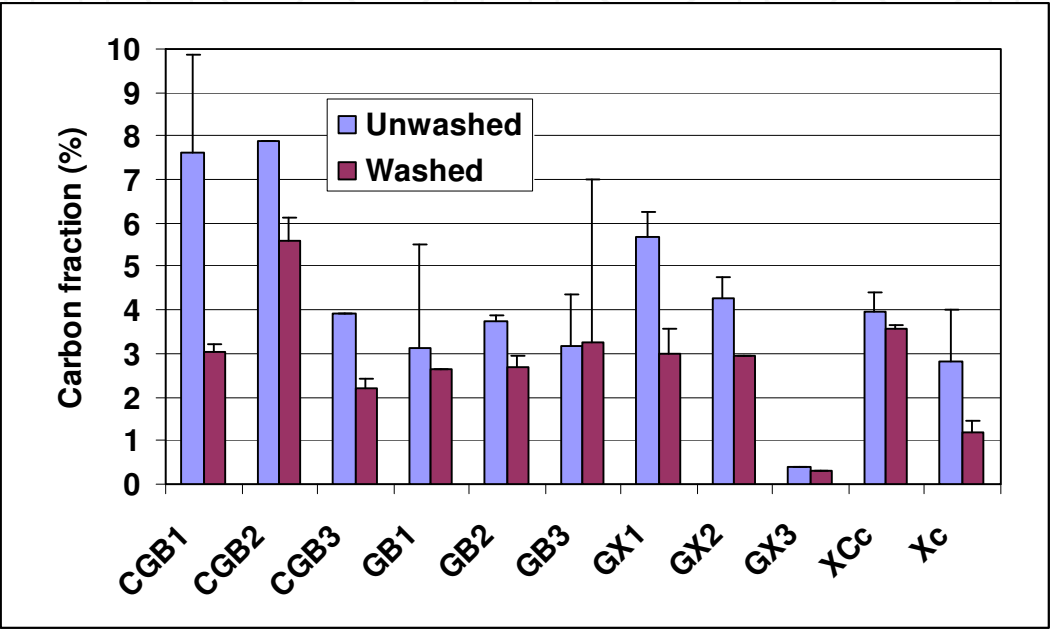
Fig. 4. Carbon fraction of biopolymer coated sand; C – chitosan, G – guar gum, B - borax, X – xanthan, c – calcium chloride.

	Phenanthrene L kg^{-1}	Pyrene L kg^{-1}
Sand	3.19 (1.87)	27.01 (5.34)
CGB1	0.4 (-)	29.54 (4.19)
CGB2	27.72 (3.07)	127.1 (23.26)
CGB3	40.64 (24.32)	118.3 (17.15)
GB2	13.18 (2.32)	68.82 (14.4)
XCc	12.8 (3.42)	106.7 (15.08)

Table 3. Average sorption coefficients of sand and sand coated by biopolymers (standard deviation in parentheses); B - borax, C - chitosan, G - guar gum, X - xanthan, c - calcium chloride.

3.2 Stability of cross-linked biopolymers under varying environmental conditions

Cross-linking agents added to biopolymers enhance their strength and decrease their biodegradability. However, the stability of biopolymers and their life span in the field may be affected by environmental conditions. The stabilities of selected cross-linked biopolymers were evaluated over extended periods (10 weeks to 6 months) in the laboratory using temperature and leaching studies to simulate accelerated weathering. Indications of degradation or loss of effectiveness served to identify potential concerns with long-term stability.

3.2.1 Biodegradability of biopolymers

A ten week evaluation of several biopolymers (Fig. 5) showed that chitosan cross-liked with guar gum and borax (CGB) and xanthan cross-linked with chitosan and calcium chloride (XCc) had the lowest evolution of CO_2; i.e., the lowest degradability. Biopolymers, especially xanthan cross-linked by guar gum, degraded faster under wet conditions and high temperatures (35^oC) than under dry conditions (Fig. 6).
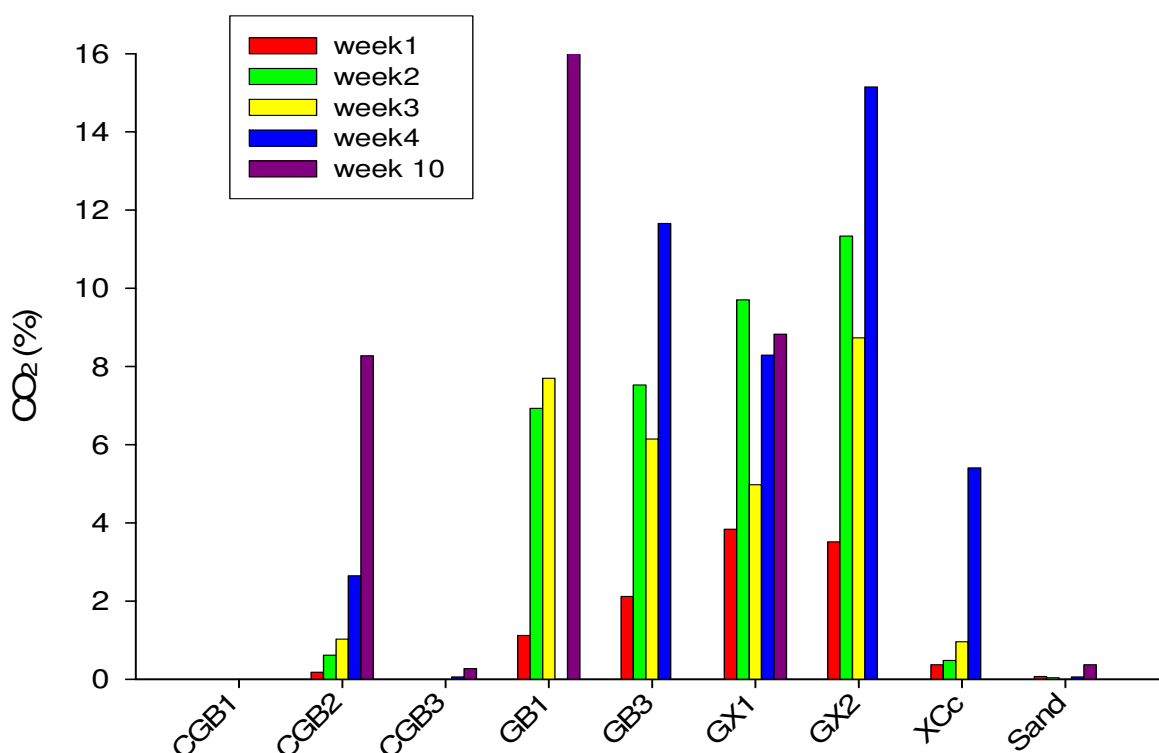
Fig. 5. Release of CO_2 (measured by GC-MS) from several cross-linked biopolymers: B - borax, C - chitosan, G - guar gum, X - xanthan, c - calcium chloride, 1 & 3 - without glutaral-dehyde, 2 - with glutaraldehyde, 3 – with NaOH

Microbial densities associated with the biopolymers likely were a result of bacteria present during manufacture of the biopolymers. Minimal increases in bacterial densities and CO_2 release over 6 months and under various conditions indicated that biopolymer-associated microbes did not contribute significantly to the degradation of some biopolymers (Fig. 7). Biopolymers with sorbed metals demonstrated decreased CO_2 release and likely minimal biodegradation compared to biopolymers without sorbed metals (Fig. 8 and 9). Obvious morphological differences in bacteria isolated from biopolymers further indicated that

different microbial consortia were associated with biopolymers as a function of metal concentration. Biodegradation of biopolymers resulted in minimal release of metal contaminants (Fig. 10).
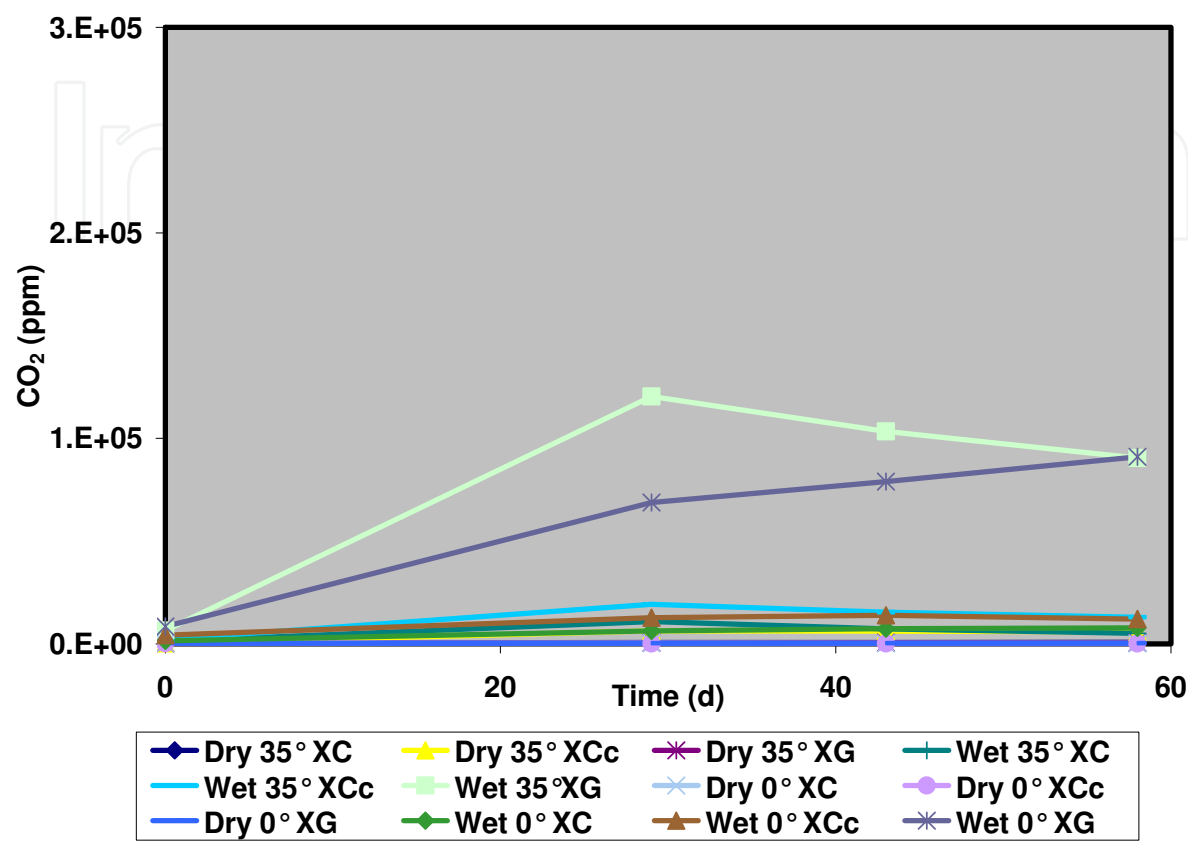

Fig. 6. Evaluation of biopolymer degradation under wet/dry conditions and different temperatures; X - xanthan, G - guar gum, C- chitosan, c - calcium chloride.
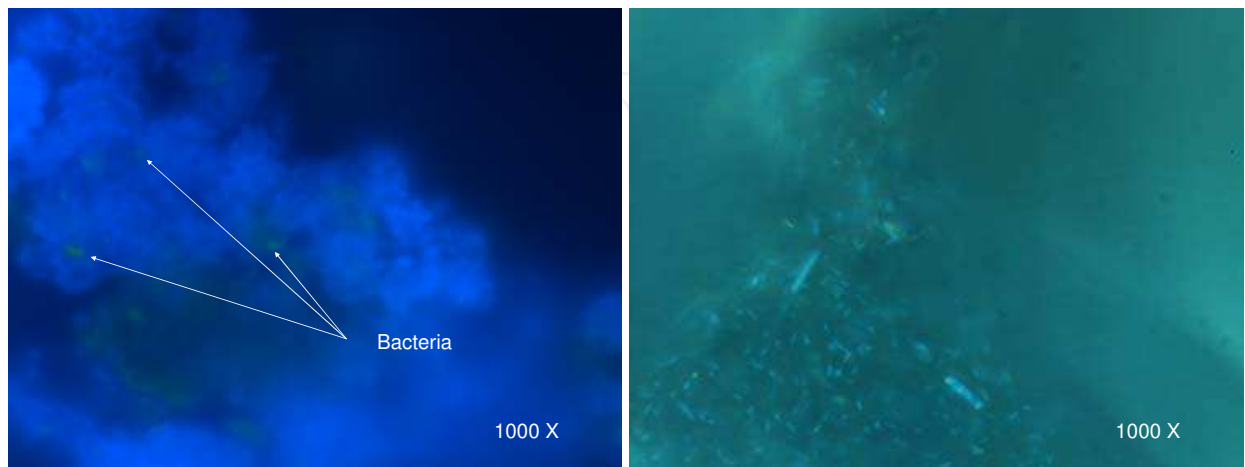

Fig. 7. Microscopic analyses of biopolymer surfaces using 4',6-diamidino-2-phenylindole (DAPI) and epifluorescence microscopy. Biopolymer XCc (left) contained fewer bacteria than CGB (right) after 6 months of contact with sediment suggesting limited biodegradation.
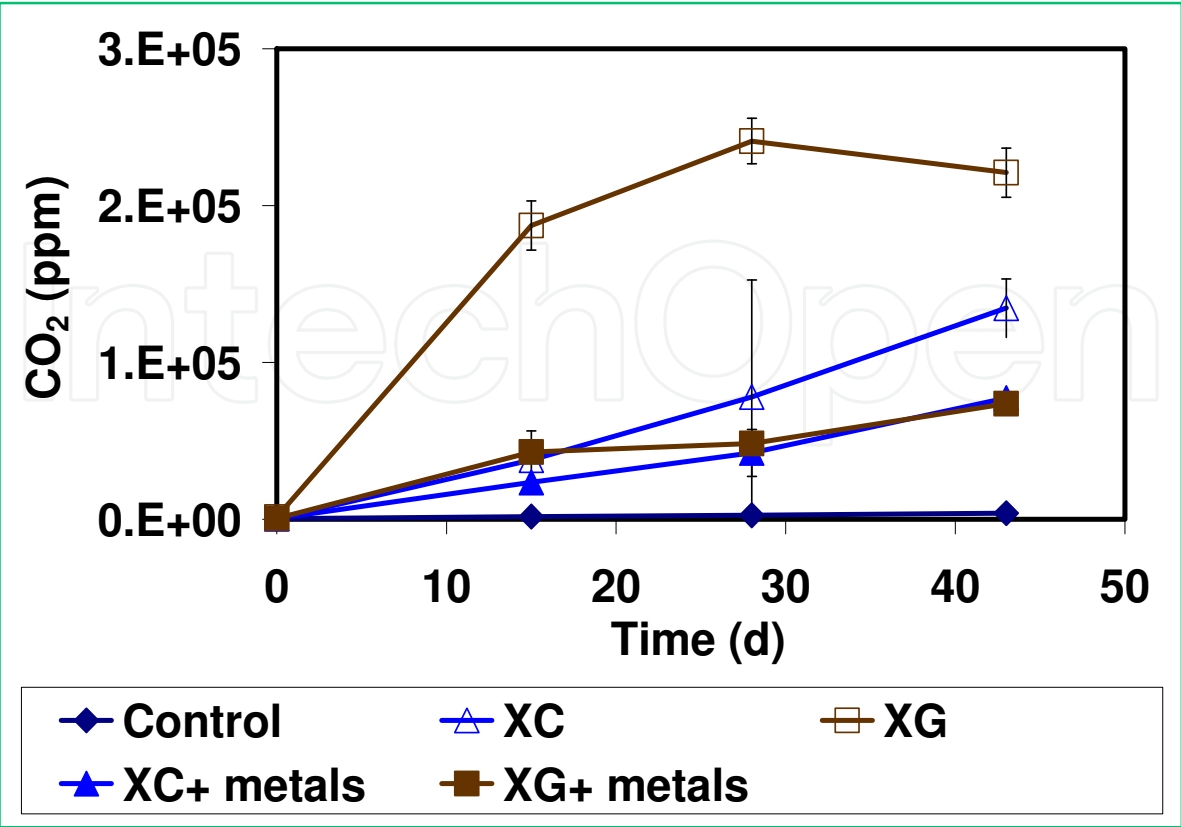
Fig. 8. Evaluation of biopolymer degradation for 45 days; X - xanthan, G - guar gum, and C-chitosan. Metal sorption of biopolymers inhibited bacterial activity.
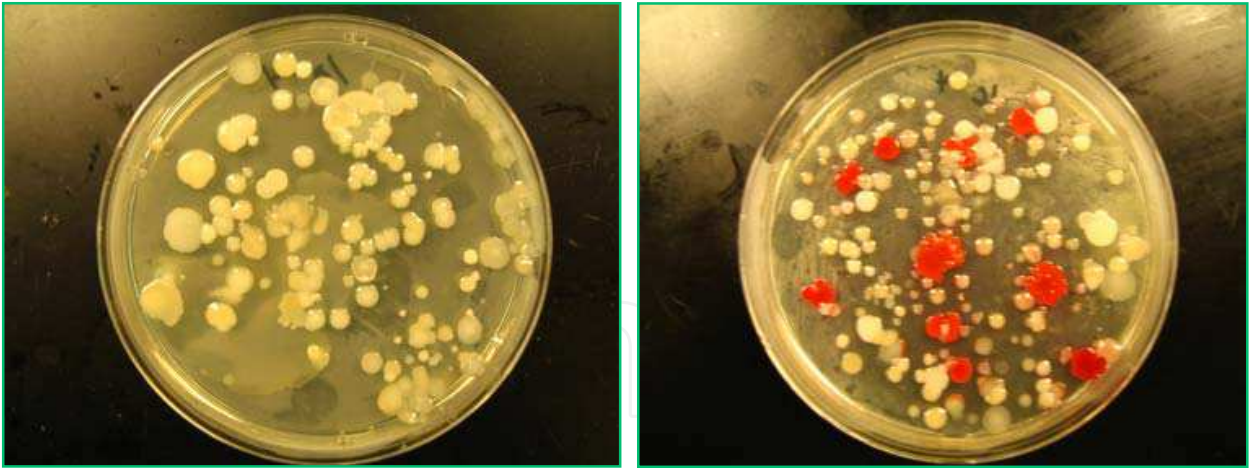
Fig. 9. Morphological differences in bacterial populations after exposure to Xanthan biopolymers without (left) and with (right) sorbed metals.

This study showed that cross-linked biopolymers have the potential to remove contaminants from the aqueous phase and to stabilize contaminants in soils/sediments. Cross-linked biopolymers vary in their susceptibility to biodegradation, with some being resistant for several months. Biopolymer degradation did not result in contaminant release during the test period. Our research showed that cross-linked biopolymers are promising for remediation, but longer periods of evaluation under field conditions are still needed.
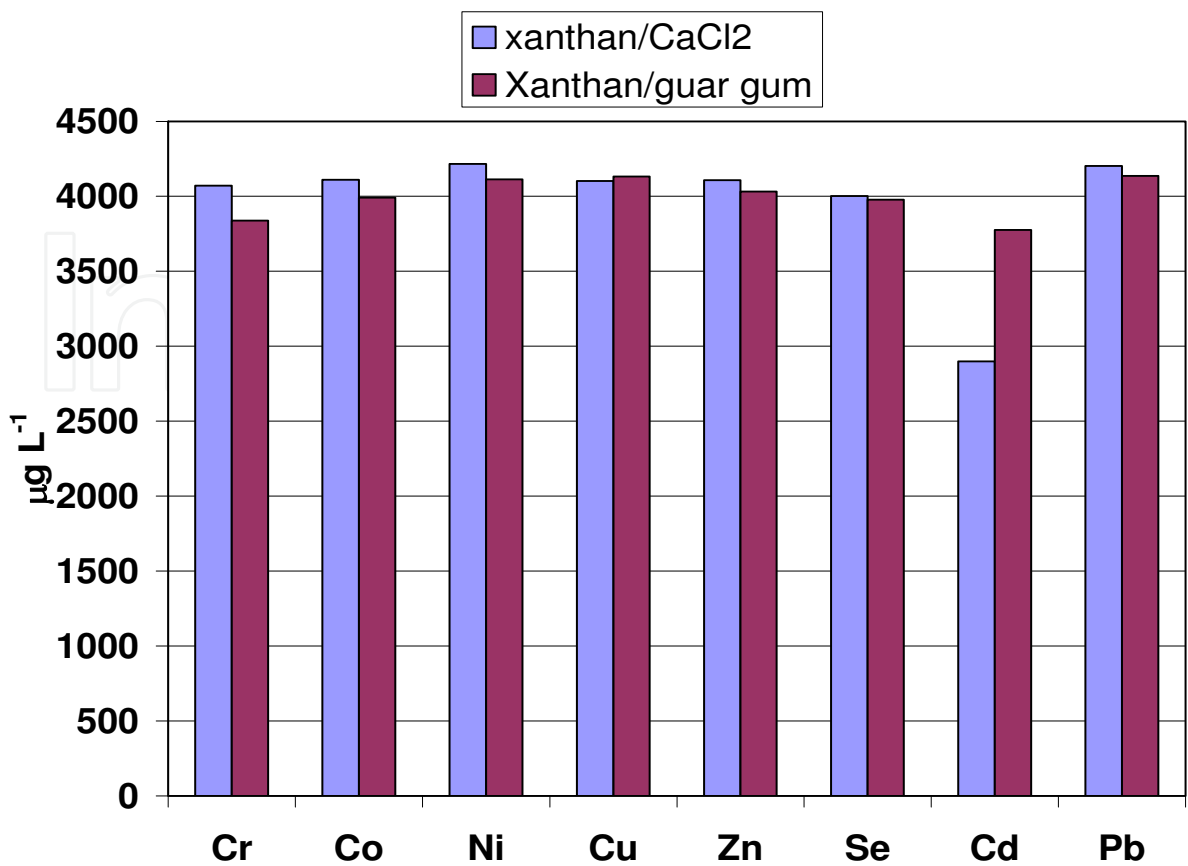
Fig. 10. Metals remaining in biopolymers after 3 months of biodegradation (initial concentration of the spike solution was 5000 µgL^{-1}).

3.3 Evaluation of biopolymer resistance to physical disturbance

Various biopolymers were cross-linked with and without coating on sand or amendments (Tab. 2). The cross-linked biopolymer products had increased viscosity and shear strength (results not shown here). They also had an evident cohesiveness, some of them looking and acting literally like "glues" when wet (Fig. 11). These physical characteristics indicate that some biopolymers have potential for use in active caps as an adhesive, binding cap materials together, and for removal of contaminants.

3.3.1 Shaker tests

The shaker suspension-simulation device was used to test the suspension resistance of sand, biopolymer coated sands, and organoclay. Five suspension thresholds were established: fine top particles disturbed, motion of top particles, cloudiness, full re-suspension of top layer, and full re-suspension of the bottom layer. The oscillations of the grid used to produce these motions were converted into shear stresses. These stresses were compared with those calculated with Shield's curve equations, which are indicators of the stability of non-cohesive particles in a bed. Full re-suspension of the bottom layer of sand was not achieved (Fig. 12). The deepest penetration into the 7cm high sand layer was 1.5 cm. The maximum speed that the motor was able to achieve was approximately 650 rpm. In the paper by Tsai and Lick, maximum speed derived from the given oscillation periods was 750 rpm (Tsai and

Lick 1986). Full re-suspension of the bottom layer may have been achieved if the motor would have reached higher speeds.

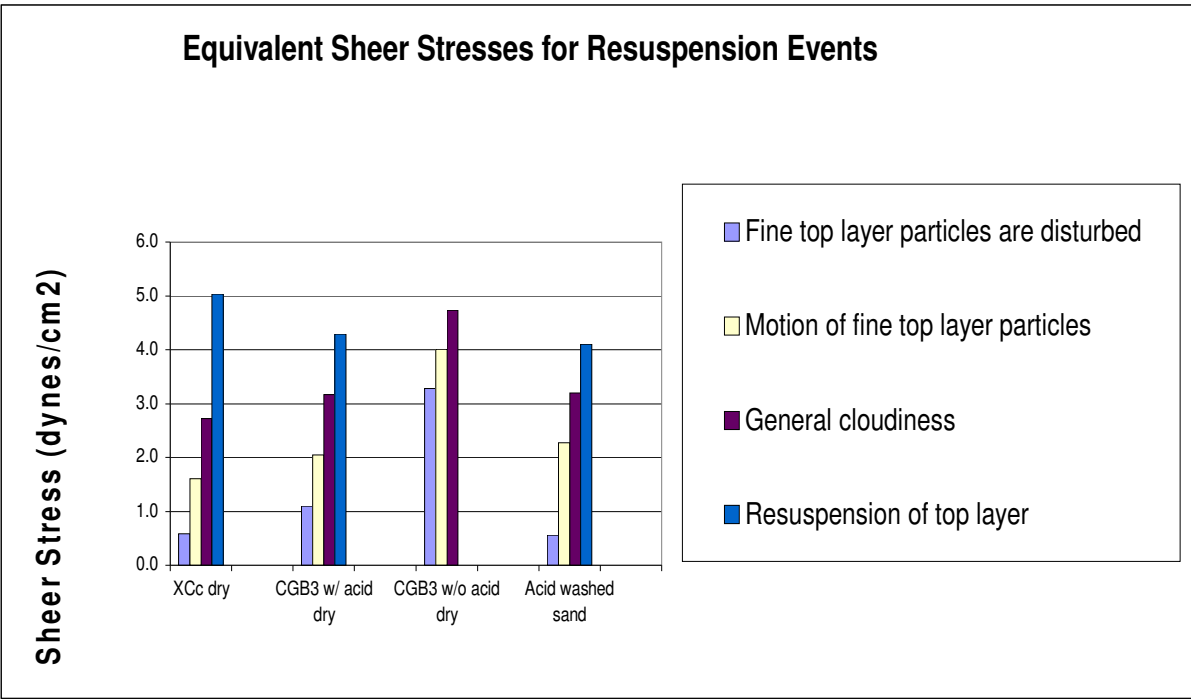Fig. 11. Adhesive product of sand coated with guar gum cross-linked by borax.

Fig. 12. Effects of equivalent sheer stresses on resuspension of sand and three types of dry and rewetted biopolymer coated sand.

Dried biopolymer coated sands CGB3 and XCc treated with addition of HCl in the preparation process performed similarly to plain sand. The biopolymer coatings in these products did not become viscous after rewetting and did not aid in preventing suspension of the sediment columns (Fig. 12). However, the dry coated sand CGB3 prepared without

HCl (Table 2) produced a viscous gel immediately upon rewetting and was resistant to suspension (Fig. 12). The gel properties of the rewetted biopolymer significantly increased the sheer stresses required for resuspension of sediments (Fig. 12). Even at maximum rotational speed very little disturbance of CGB3 was observed and the top layer was never resuspended (Fig. 12).

Additional suspension experiments were conducted to test the stability of multiple biopolymer materials when placed in viscous slurry rather than first drying and then rewetting. The results of these tests are displayed in Fig. 13. The slurry products performed very well in the suspension experiments. Initial oscillations of the grid caused the uppermost portions of the slurries to pulse vertically but no sloughing of the samples occurred. Increased sheer stresses resulted in minor sloughing of small particles but no resuspension occurred. Sand with biopolymers, e.g., xanthan cross linked with guar gum (XG), was suspension resistance even at a speed of 11 m/s (Figs. 14 & 15). Mixtures of biopolymer XG, sand, and other amendments such as organoclay and/or apatite were also suspension resistant at a speed 11 m/s (Fig. 16). The significant resistance of the slurry products to suspension shows promise for future applications as a stand-alone active cap or as armament for other amendments.

Organoclay (PM-199) without biopolymers was not suspension resistant. If placed in a flowing aquatic environment, a cap of organoclay would erode like a plain sand cap (Fig. 17).
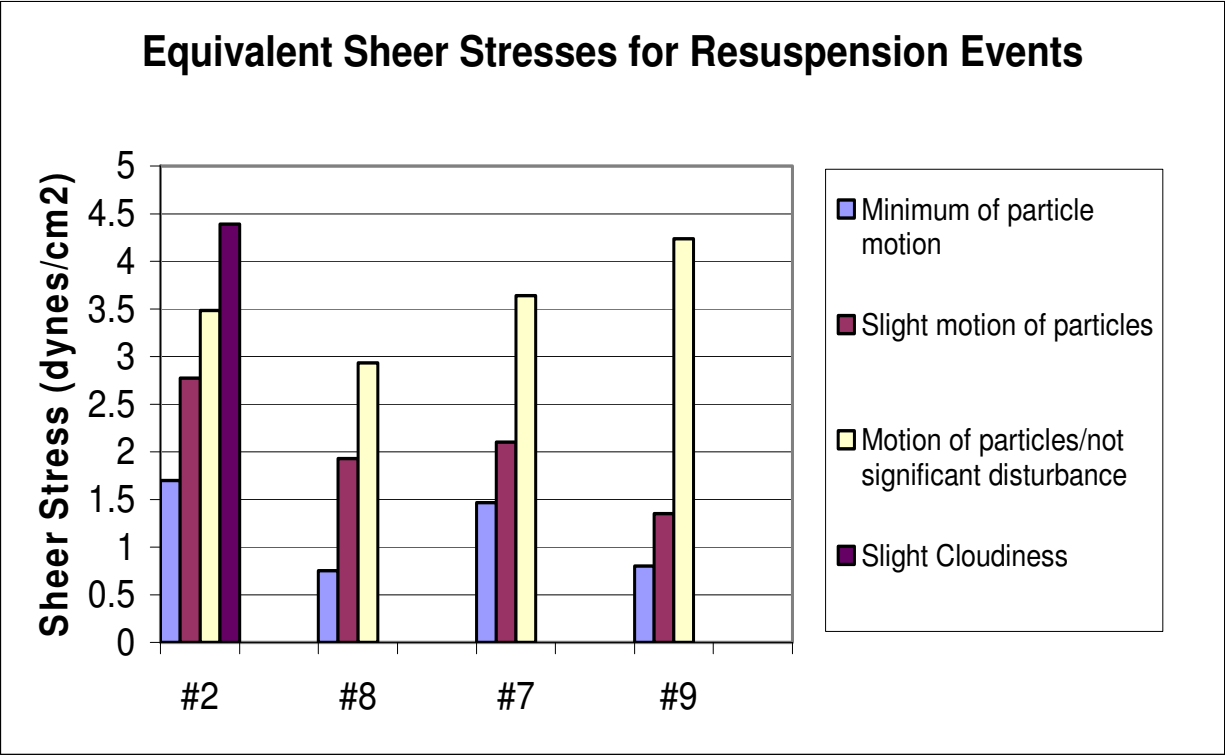

Fig. 13. Effects of equivalent sheer stresses on sand and slurries of biopolymer coated sand: 2 – sand with chitosan/guar gum/borax, 7 – sand with xanthan/guar gum and apatite, 8 - sand with xanthan/guar gum and organoclay (PM-199), 9 - sand with xanthan/guar gum and apatite, and organoclay.
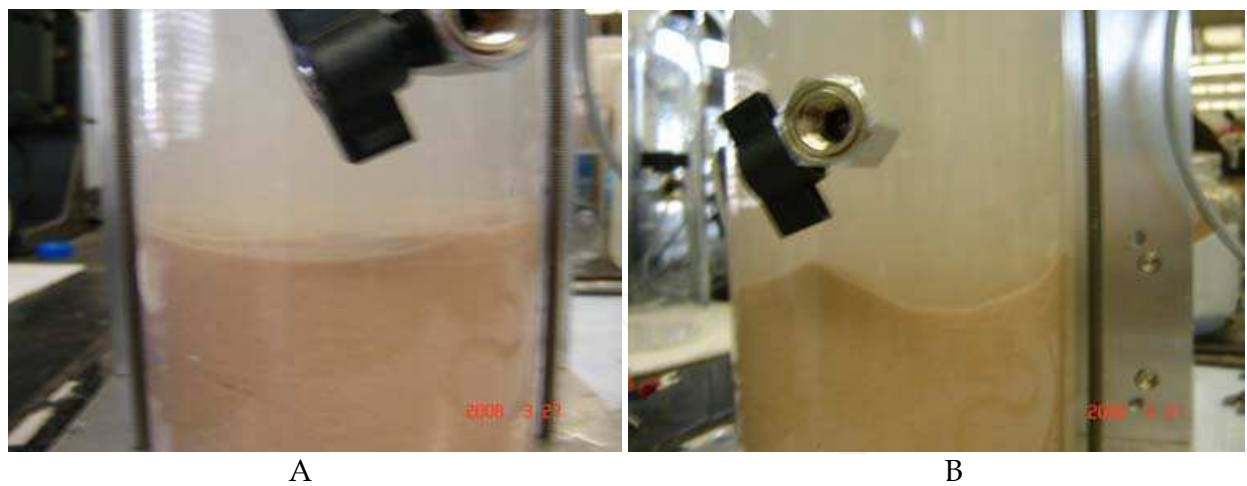
Fig. 14. Plain sand was easily resuspended at very low speed (3.7 m/s) (A) and exhibited marked erosion at higher speed (11 m/s) (B).

Fig. 15. Coated sand with xanthan and guar gum did not exhibit erosion at speeds of 3.7 m/s (A) or 11m/s (B).

Fig. 16. Sand and organoclay (PM-199) mixed with the biopolymers xanthan and guar gum did not show erosion at speeds of 3.7m/s (A) or 11m/s (B).

A   B

Fig. 17. Resuspension of organoclay (PM-199) leading to cloudiness (A) and surface suspension (B).

3.3.2 Adjustable Shear Stress Erosion and Transport (ASSET) flume

The materials evaluated in the shaker and ASSET flume tests are listed in Tab. 4 where they have been assigned product numbers. The products included:

- #4 XCc - sand and xanthan/chitosan cross-linked with calcium chloride and glutaraldehyde,
- #5 XG - sand and 2.5% guar gum cross-linked with xanthan (Kelzan brand),
- #6 XG Coyote - sand and 5% guar gum cross-linked with xanthan (Coyote brand),
- #6 XG Kelzan - sand and 5% guar gum cross-linked with xanthan (Kelzan brand),
- #7 AXG - sand, 12.5% apatite and 5% guar gum cross-linked with xanthan (Kelzan brand),
- #8 OXG - sand,12.5% organoclay, and 5% guar gum cross-linked with xanthan (Kelzan brand); and
- #9 XG/AO - sand, 12.5% organclay, 12.5% apatite, and 5% guar gum cross-linked with xanthan (Kelzan brand).

Erosion rates as a function of shear stress and depth were obtained for six of the seven materials after 2, 10, and 175 days of consolidation at shear stresses of 0.25, 0.5, 0.75, 1.0, 1.5, 2.0, 3.0 and 4.0 N/m². After preliminary tests of the #7 AXG material at 2 and 5 days, the sample did not show promise as an erosion resistant cap material and was dropped from further testing. The ASSET flume erosion tests enabled stability evaluation of nearly the entire thickness of the cap (~10 cm) under simulated flow conditions that ranged from quiescent to the shear environment in extreme storm events. The erosion rate ratio analysis is used to compare average erosion behavior at distinct intervals within a core. An example of how the two methods correlate is shown for the #9 XG/AO and #8 OXG samples after 10 days of consolidation (Fig 18). Graphics A and B in Fig. 18 show that erosion decreases with increasing depth in the # 9XG/OA cap material while graphics C and D show increased erosion in the center of the core with the most erosion resistant layer at the bottom.

The individual erosion behavior of the six dominant cap materials is shown in Fig. 19. The six graphics compare the erosion behavior at 2, 10 and 175 days of consolidation at each erosion inverval as well as the core average. This enables the evaluation of the erosion behavior of each cap material as a function of consolidation time and depth within the core

sample. For example, the #4 XCC and #9 XG/OA samples display a general hardening or resistance to erosion with increasing core age. Both samples also show that each core became more stable at depth at all ages except for the second depth interval in the 2 day #9 XG/OA sample. It is important to note that the scale on the #9 XG/OA plot is expanded by two orders of magnitude and shows that the oldest, 175 days of consolidation, sample is the most stable or erosion resistant core of all. The #6 XG Kelzan sample shows the opposite trend in that it becomes softer or less erosionaly stable as the sample ages. This same sample shows that the surface layer at all ages is always the easiest to erode with general, but not consistent trends, of hardening at depth. The remaining cores, #5 XG, #6 XG Coyote, and #8 OXG, show inconsistent erosion behavior with sample age and depth within the core.

The core average erosion rates for the six primary materials are compared at 2, 10, and 175 days of consolidation along with the time average erosion rate for each material (Fig 20). Sand mixed with XG (xanthan gum) Coyote and XG Kelzan generally became more difficult to erode with depth for all shear stresses. Erosion was in the form of small aggregates (~0.5-2 mm) that often formed small runnel-like features in the surface of the core parallel to the flow path and left a fairly uniform and smooth surface layer. The material was very cohesive and exhibited behaviors consistent with naturally cohesive sediments (Roberts et al, 1998).
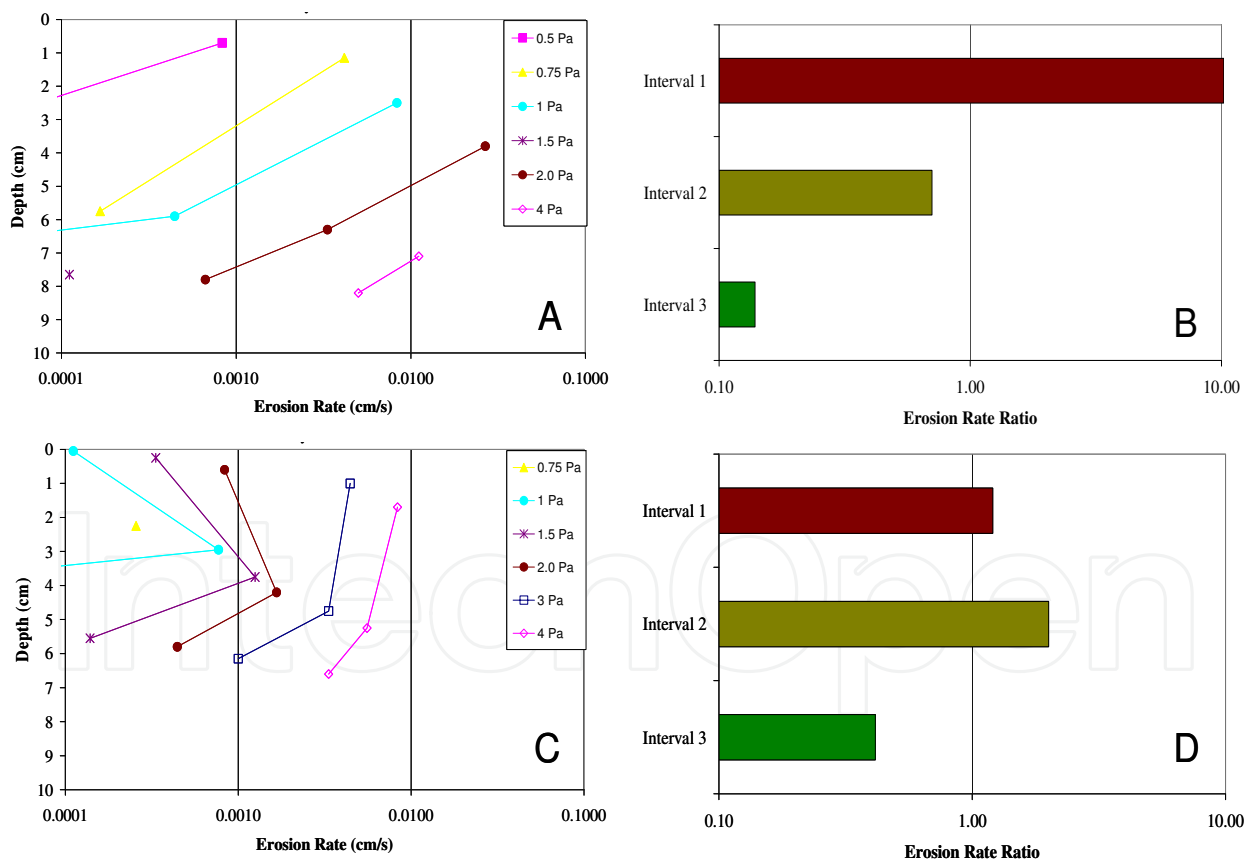

Fig. 18. (A) #9 XG/AO 10 day consolidation erosion rate as a function of depth at shear stresses of 0.5, 0.75, 1.0, 1.5, 2.0, and 4.0 Pa. (B) #9 XG/AO 10 day consolidation erosion rate ratio for the 3 erosion intervals. (C) #8 OXG 10 day consolidation erosion rate as a function of depth at shear stresses of 0.75, 1.0, 1.5, 2.0, 3.0, and 4.0 Pa. (D) #8 OXG 10 day consolidation erosion rate ratio for the 3 erosion intervals.

Sample ID	Critical Shear Stress Range (Pa)	Erosion Rate Range at 1.0 Pa (cm/s)	Erosion Rate Generally Decreases with Depth
2 Day Consolidation			
#4 XCC	0.17 - 0.51	0.0083 - 0.013	Yes
#5 XG	0.73 – 0.99	0.00011 - 0.00067	Yes
#6 XG Coyote	0.86 – 1.90	$<10^{-4}$ - 0.00022	Yes
#6 XG Kelzan	0.73 - 1.73	$<10^{-4}$ - 0.00033	Yes
#7 AXG	0.28 – 0.75	0.00067 – 0.0083*	No, center layer easiest to erode
#8 OXG	0.30 – 0.73	0.00017 – 0.0033	No, easier with depth except for second depth interval
#9 XG/AO	0.30 – 1.2	$<10^{-4}$ - 0.0033	No, center layer easiest to erode although bottom layer was most erosion resistant
10 Day Consolidation			
#4 XCC	0.28 – 0.71	0.00095 - 0.00278	Yes
#5 XG	0.73 – 1.45	$<10^{-4}$ - 0.00022	Yes
#6 XG Coyote	0.28 – 0.73	0.00017 - 0.002	No, surface and bottom layers easier to erode
#6 XG Kelzan	0.73 – 1.65	$<10^{-4}$ - 0.00067	Yes
#7 AXG (5-days)	0.25 – 0.75	0.00067 – 0.0035	No, center layer easiest to erode
#8 OXG	0.60 – 1.36	$<10^{-4}$ - 0.00077	No, center layer easiest to erode
#9 XG/AO	0.28 – 1.45	$<10^{-4}$ - 0.00083	Yes
175 Day Consolidation			
#4 XCC	0.98 – 1.06	$<10^{-4}$ - 0.00011	Yes
#5 XG	0.65 – 1.61	$<10^{-4}$ - 0.0005	Yes
#6 XG Coyote	0.61 – 0.98	0.00011 - .000056	Yes
#6 XG Kelzan	0.73 – 0.98	0.00011 - .000044	Yes, but second depth interval was most erosion resistant
#8 OXG	0.24 – 0.86	0.00022 - .00303	Yes
#9 XG/AO	0.73 – 3.3	$<10^{-4}$ - 0.00033	Yes

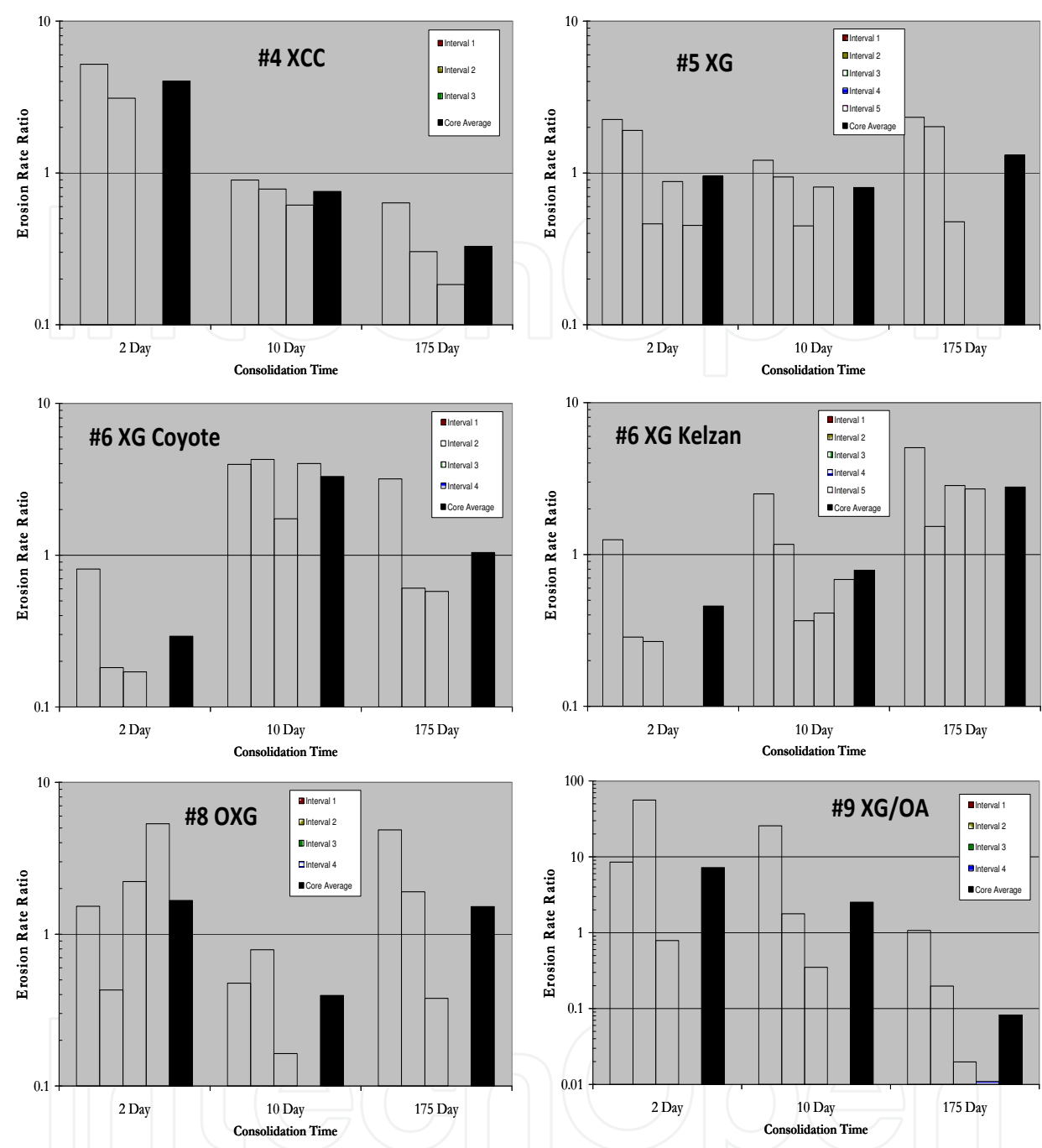Table 4. Summary of erosion properties for 2, 10 and 175 days of consolidation.

Fig. 19. Erosion rate ratio for six primary cap materials that compares all erosion intervals and the core average erosion at consolidation times of 2, 10, and 175 days.

The erosive behavior of AXG differed from that of the other materials (Tab. 4). The erosion resistance of some materials increased with time as indicated by core average critical shear stress shown in Fig. 20. Comparisons between the two and 10 day consolidation periods showed that XCC, XG (2.5% biopolymer), XG Kelzan, OXG Kelzan, and XG/AO Kelzan became harder to erode as they became more consolidated (Tab. 4 and Fig. 20 and 21). Xanthan/guar gum mixed with apatite and organoclay showed long term (175 day) physical stability (Fig. 20 and 21). The critical shear stress for this material exceeded 2Pa in the 175 day consolidation test indicating its promise as a cap material (Fig. 21).
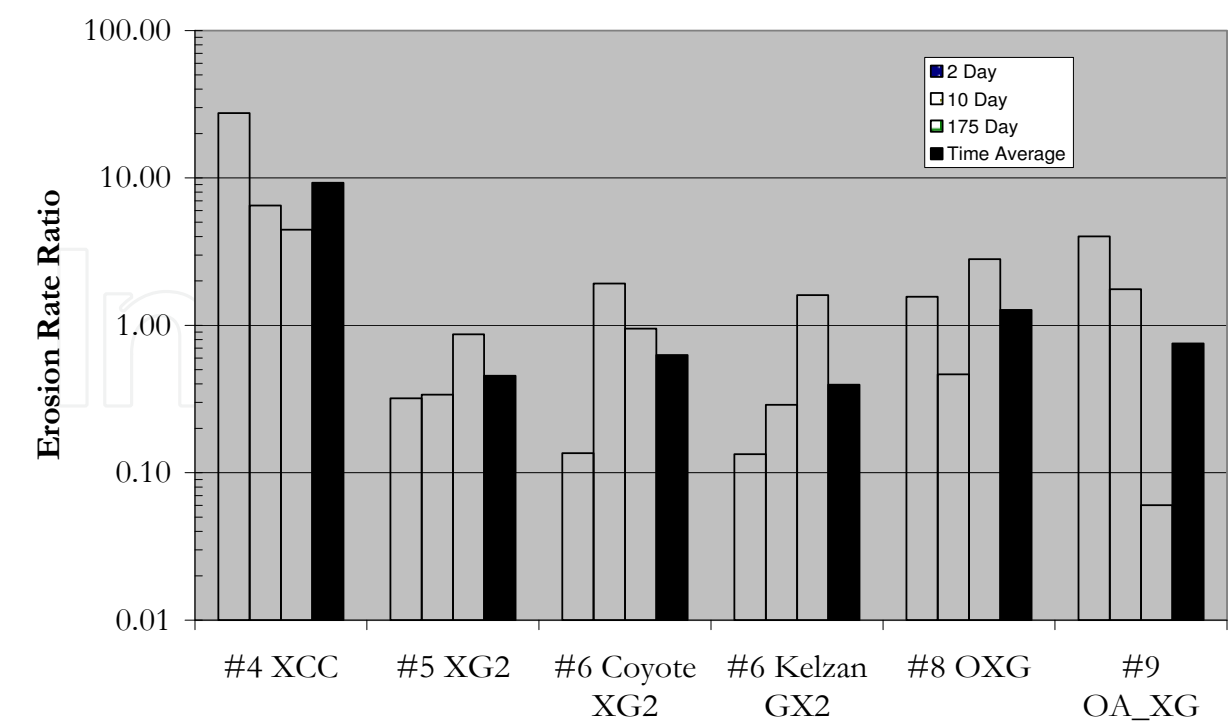
Fig. 20. Comparison of core average erosion rates at 2, 10, and 175 day consolidation including the time average of all three.
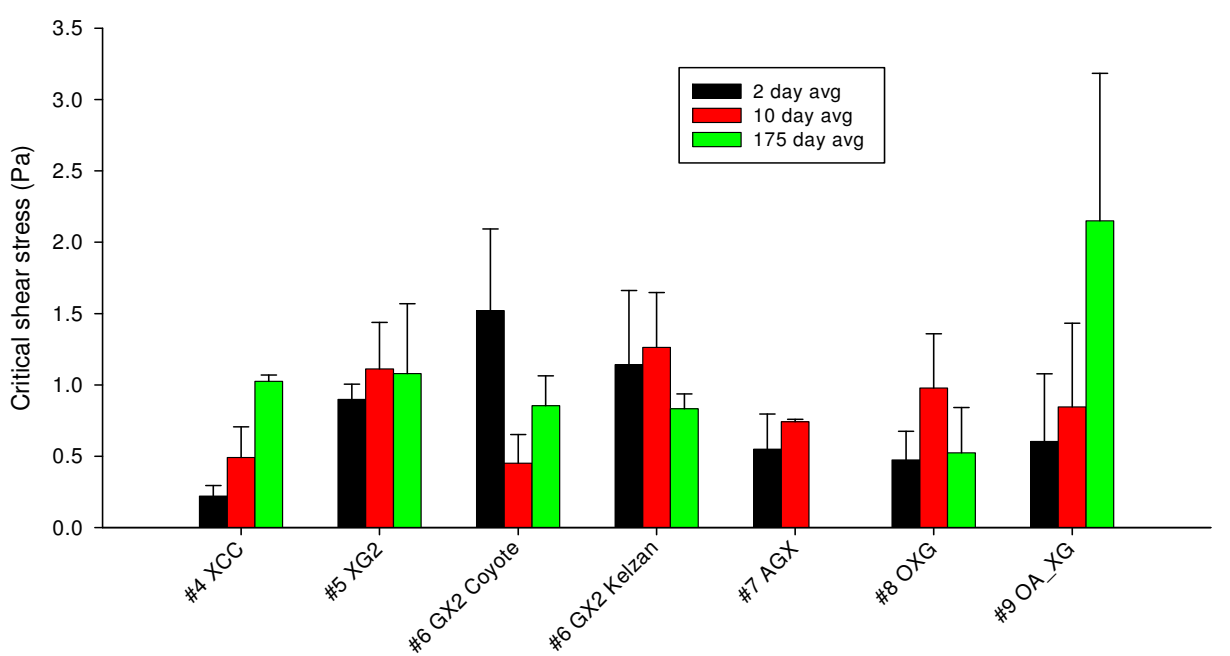

Fig. 21. Critical shear stress comparison among biopolymer materials at 2, 10, and 175 days. Each value is an average of measurements taken at two to five different depths in a core sample. Error bars represent standard deviations.

4. Conclusions

The biopolymer materials tested for possible application in remediation of contaminated soils or sediments showed potential for immobilization of metals and some organic contaminants. Most of the tested products demonstrated good erosion resistance capabilities in the laboratory. Slurry mixtures consisting of xanthan and guar gum with entrained amendments and sand showed the greatest resistance to erosion. Addition of highly metal or organic sorptive amendments (e.g., apatite or organoclays) to biopolymer products should significantly augment the sequestering capabilities of the products and increase their remedial applicability and efficiency. The results from this laboratory evaluation of biopolymers were consistent with a recently conducted pilot study in which xanthan and guar gum were evaluated in the field (Knox et al., 2009). Both laboratory and field studies showed that guar gum cross-linked with xanthan (Kelzan) became less resistant to erosion after two months. The application of xanthan/guar gum in the field as the top layer of active caps is beneficial for a short time for erosion resistance. This mixture also reduced sediment suspension during cap construction and caused the rapid settling of other amendments that were placed below the biopolymer layer. Biopolymers can also increase the pool of carbon in the sediment beneath caps and lower the release of metals and other elements, especially P, in comparison with apatite only (Knox et al., 2009). However, more research is needed on the type of biopolymers applied to caps and methods for delivering biopolymers to the cap. Further research is especially needed on the biodegradability of biopolymers under extreme aquatic conditions (e.g., high summer temperature, changing ratios of Fe-S-P in sediment pore and surface water, and other factors). Finally, the applicability of biopolymer products in active capping technology is also dependent on the effects of these products on benthic organisms. Although biopolymers are nontoxic, the viscous matrix produced by biopolymers may have the potential to physically entrap or suffocate burrowing organisms (Paller & Knox, in press).

5. Acknowledgment

6. References

Araujo, M.M. & Teixeira, J.A. (1997). Trivalent Chromium Sorption on Alginate Beads. *Int. Biodeter. Biodegr.* 40(1): 63-74.

Cadmus, MC., Jackson, J.K, Burton, K.A. Plattner, R.D. & Slodki, M.E. (1982). Biodegradation of xanthan gum by *Bacillus* sp. *Appl. Enviorn. Microbiol.* 44-5-11.

Bassi, R.; Prasher, S.O. & Simpson, B.K. (1999). Remediation of metal-contaminated leacgate using chitosan flakes. *Eviron. Tech.* 20:1177-1182.

Chen, D., Lewandowski, Z., Roe, F. & Surapanemi, P. (1993). Diffusivity of Cu^{2+} in calcium alginate gel beads. *Biotechnol. Bioeng.* 41: 755-760.

Chen, J. & Yen, T. F. (1990). Transport of Microorganisms to Enhance Soil and Groundwater Bioremediation, Proceedings, Hazmacon1990 (T. Burszynski, ed.) ABAG, San Francisco, Vol. II, pp. 95-100.

Deans, J.R. & Dixon, B.G. (1992). Uptake of Pb $^{2+}$ and Cu $^{2+}$ by novel biopolymers. *Water Res.* 26 (4): 469-472.

Etemadi, O.; Petrisor, I.G.; Kim, D.; Wan, M.-W. & Yen, T.F. (2003). Stabilization of Metals in Subsurface by Biopolymers: Laboratory Drainage Flow Studies. *Soil & Sediment Contamination: An International Journal* 12 (5): 647-661

Fiol, N.; Poch, J. & Villaescusa, I. (2004). Chromium (VI) uptake by grape stalks wastes encapsulated in calcium alginate beads: equilibrium and kinetics studies. *Chemical Speciation and Bioavailability* 16(1/2): 25-33.

Francis, A.J. & Dodge, C.J. (1993). Influence of complex structure on biodegradation of iron-citrate complexes. *Appl. Environ. Microbiol.* 59: 109-113.

Jepsen, R..; Roberts, J. & Lick, W. (1996). Effects of Bulk Density on Sediment Erosion Rates, *Water, Air, and Soil Pollution,* 99: 21-31.

Jepsen, R.; Roberts, J. & Lick, W. (1997). Long Beach Harbor Sediment Study, Report Submitted to the U.S. Army Corps of Engineers, DACW09-97-M-0068

Khachatoorian, R.; Petrisor, I.G. & Yen, T.F. (2004). Prediction of Plugging Effect of Biopolymers Using Their Glass Transition Temperatures. *Journal of Petroleum Science & Engineering* 41: 243-251.

Kartal, S.N. & Imamura, Y. (2004). Removal of copper, chromium, and arsenic from CCA-treated wood onto chitin and chitosan. *Bioresource Technology* 96(3): 389-392.

Kim, D.; Petrisor, I.G. & Yen, T.F. (2004). Geopolymerization of biopolymers; a preliminary inquiry. *Carbohydrate Polymers,* 56: 213-217.

Kim, D.; Petrisor, I.G. & Yen, T.F. (2005). Evaluation of Biopolymer-Modified Concrete Systems for Disposal of Cathode Ray Tube Glass. *J. Air & Waste Manage. Assoc.,* 55: 961-969.

Knox, A.S.; Paller, M.H.; Reible, D.D. & Petrisor, I.G. (2006). Innovative in-situ remediation of contaminated sediments for simultaneous control of contamination and erosion. Annual Report 2007, WSRC-RP-2006-01149.

Knox, A.S.; Paller, M.H.; Petrisor, I.G. & Reible, D.D. (2007). Sequestering agents for metal immobilization – application to the development of active caps in fresh and salt water sediments. Conference Proceedings of the Fourth International Conference on Remediation of Contaminated Sediments, Savannah, Georgia, January 22-25, 2007, Battelle Press: ISBN 978-1-57477-159-6.

Knox, A.S.; Dixon, K.L.; Paller, M.H.; Reible, D.D.; Roberts, J. & Petrisor, I.G. (2008a). Innovative in-situ remediation of contaminated sediments for simultaneous control of contamination and erosion. Annual Report 2008, SRNL-RP-2008-01216.

Knox, A.S.; Paller, M.H.; Reible, D.D.; Ma, X. & Petrisor, I.G. (2008b). Sequestering Agents for Active Caps – Remediation of Metals and Organics, Soil and Sediment Contamination: An International Journal, 17(5): 516-532.

Knox, A.S.; Paller, M.H.; Dixon, K.L.; Reible, D.D. & Roberts, J. (2009). Innovative in-situ remediation of contaminated sediments for simultaneous control of contamination and erosion. Annual Report 2009, SRNL-RP-2009-01497.

Kostal, J.; Mulchandani, A.; Gropp, K.E.; & Chen, W. (2003). A Temperature Responsive Biopolymer for Mercury Remediation. *Environ. Sci.Technol.* 37: 4457-4462.

Lehman, R.M.; Colwell, F.S. & Bala, G.L. (2001). Attached and Unattached Microbial Communities in a Simulated Basalt Aquifer under Fracture- and Porous-Flow Conditions. Appl. Environ. Microbiol. 67: 2799-2809.

McNeil, J.; Taylor, C. & Lick, W. (1996). Measurements of the Erosion of Undisturbed Bottom Sediments with Depth, *Journal of Hydraulic Engineering.* 122 (6): 316-324.

Palermo, M.R.; Maynord, S.; Miller, J. & Reible, D.D. (1998). Guidance for in-situ subaqueous capping of contaminated sediments. Chicago, Great Lakes National Program Office.

Paller, M.H. & Knox, A.S. (2010). Amendments for the remediation of contaminated sediments: Evaluation of potential environmental impacts. *Sci. Total Environ.* (in press).

Prabhukumar, G.; Matsumoto, M.; Mulchandani, A. & Chen W. (2004). Cadmium Removal from Contaminated Soil by Tunable Biopolymers. *Environ Sci. Technol.* 38: 3148-3152.

Randall, J.M.; Randall, V.G; McDonald, G.M.; Young, R.N. &Marsi, M.S. (1979). Removal of trace quantities of nickel from solution. *J. Appl. Polym. Sci.* 23: 727-732.

Reible, D.D.; Lampert, D.; Constant, W.D.; Mutch, R.D. & Zhu, Y. (2006). Active Capping Demonstration in the Anacostia River, Washington, DC, Remediation: The Journal of Environmental Cleanup Costs, Technologies and Techniques, 17 (1): 39-53.

Rhodes, J. & Roller, S. (2000). Antimicrobial actions of degraded and native chitosan against spoilage organisms in laboratory media and foods. *Appl. Environ. Microbiol.* 66: 80-86.

Roberts, J.; Jepsen, R.; Gotthard, D. & Lick, W. (1998). Effects of Particle Size and Bulk Density on Erosion of Quartz Particles. *Journal of Hydraulic Engineering.* 124(12): 1261-1267.

Roberts, J. & Jepsen, R. (2001). Development for the Optional Use of Circular Core Tubes with the High Shear Stress Flume. SNL report to the US Army Corps of Engineers, Waterways Experiment Station.

Roberts, J.; Jepsen, R. & James, S. (2003). Measurement of Sediment Erosion and Transport with the Adjustable Shear Stress Erosion and Transport Flume. *Journal of Hydraulic Engineering.* 129(11): 862-871.

Schlichting, H. (1979). Boundary-Layer Theory. Seventh Edition, McGraw-Hill. Stewart, T.L., Fogler, H.S. 2001. Biomass Plug Development and Propagation in Porous Media. Biotechnology and Bioengineering, 5: 353-363.

Tsai, C-H. & Lick, W. (1986). A portable device for measuring sediment resuspension. J. Great Lakes Res. 12(4): 314-321.

Turick, C.E.; Tisa, L.S. & Caccavo, F. Jr. (2002). Melanin production and use as a soluble electron shuttle for Fe(III) oxide reduction and as a terminal electron acceptor by *Shewanella algae* BrY. *Appl. Environ. Microbiol.* 68:2436–2444.

Udaybhaskar, P.; Iyengar, L. & Prabhakara Rao, A.V.S. (1990). Hexavalent chromium interaction with chitosan. *J. Appl. Polym. Sci.* 39: 739-747.

Wan, M.-W.; Petrisor, I.G.; Lai, H.-T.; Kim, D. & Yen, T.F. (2004). Copper adsorption through chitosan immobilized on sand to demonstrate the feasibility for in situ soil decontamination. *Carbohydrates Polymers* 55: 249-254
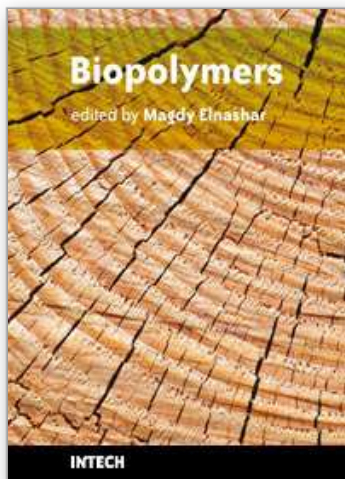
Biopolymers

Edited by Magdy Elnashar

ISBN 978-953-307-109-1

Hard cover, 612 pages

Publisher Sciyo

Published online 28, September, 2010

Published in print edition September, 2010

Biopolymers are polymers produced by living organisms. Cellulose, starch, chitin, proteins, peptides, DNA and RNA are all examples of biopolymers. This book comprehensively reviews and compiles information on biopolymers in 30 chapters. The book covers occurrence, synthesis, isolation and production, properties and applications, modification, and the relevant analysis methods to reveal the structures and properties of some biopolymers. This book will hopefully be of help to many scientists, physicians, pharmacists, engineers and other experts in a variety of disciplines, both academic and industrial. It may not only support research and development, but be suitable for teaching as well.

How to reference

In order to correctly reference this scholarly work, feel free to copy and paste the following:

A.S. Knox, I.G. Petrisor, C.E. Turick, J. Roberts, M.H. Paller, D.D. Reible and C.R. Forrest (2010). Life Span of Biopolymer Sequestering Agents for Contaminant Removal and Erosion Resistance, Biopolymers, Magdy Elnashar (Ed.), ISBN: 978-953-307-109-1, InTech, Available from: http://www.intechopen.com/books/biopolymers/life-span-of-novel-biopolymer-sequestering-agents-for-organic-and-inorganic-contaminants-

INTECH
open science | open minds